

OPEN ACCESS


IOP Publishing

Journal of Physics A: Mathematical and Theoretical

J. Phys. A: Math. Theor. 51 (2018) 365306 (18pp)

<https://doi.org/10.1088/1751-8121/aad3e6>

How to suppress dark states in quantum networks and bio-engineered structures

Thao P Le^{1,6} , Ludovica Donati^{2,6}, Simone Severini^{3,4}
and Filippo Caruso⁵ 

¹ Department of Physics and Astronomy, University College London, Gower Street, London WC1E 6BT, United Kingdom

² Department of Mechanical Engineering, University of Florence, via S. Marta 3, 50139 Florence, Italy

³ Department of Computer Science, University College London, Gower Street, London WC1E 6BT, United Kingdom

⁴ Institute of Natural Sciences, Shanghai Jiao Tong University, No. 800 Dongchuan Road, Minhang District, Shanghai 200240, People's Republic of China

⁵ LENS, QSTAR, and Department of Physics and Astronomy, University of Florence, via G. Sansone 1, I-50019 Sesto Fiorentino, Italy

E-mail: thao.le.16@ucl.ac.uk and ludovica.donati@stud.unifi.it

Received 18 March 2018, revised 8 July 2018

Accepted for publication 17 July 2018

Published 2 August 2018



Abstract

Transport across quantum networks underlies many problems, from state transfer on a spin network to energy transport in photosynthetic complexes. However, networks can contain *dark subspaces* that block the transportation, and various methods used to enhance transfer on quantum networks can be viewed as equivalently avoiding, modifying, or destroying the dark subspace. Here, we exploit graph theoretical tools to identify the dark subspaces and show that *asymptotically almost surely* they do not exist for large networks, while for small ones they can be suppressed by properly perturbing the coupling rates between the network nodes. More specifically, we apply these results to describe the recently experimentally observed and robust transport behaviour of the electronic excitation travelling on a genetically-engineered light-harvesting cylinder (M13 virus) structure. We believe that these mainly topological tools may allow us to better infer which network structures and dynamics are more favourable to enhance transfer of energy and information towards novel quantum technologies.

⁶ Authors to whom any correspondence should be addressed.



Original content from this work may be used under the terms of the [Creative Commons Attribution 3.0 licence](https://creativecommons.org/licenses/by/3.0/). Any further distribution of this work must maintain attribution to the author(s) and the title of the work, journal citation and DOI.

Keywords: quantum networks, transport, network structure, dynamics, bio-engineered structures

(Some figures may appear in colour only in the online journal)

1. Introduction

Understanding the mechanisms of optimal transport of various quantities, such as energy or information, across some underlying topology is fundamental to many problems in physics and beyond (see, for instance [1–3], and references therein). Networks can be used to model quantum channels: for example, states can be transferred along spin chains [4, 5]. In these studies, the aim is perfect state transfer and there tends to be a fixed Hamiltonian that drives the transfer. Controllability of networks asks what kind of possibly time-dependent interactions—which then affects the connectivity structure of the network—will enable any state to be transferred [6]. More recently, quantum network theory has also been applied to model how energy is transferred through biological photosynthetic complexes [7–14] and over more abstract complex networks [15–17]. There are numerous factors that need to be considered in order to achieve optimal transport: the dynamics of the network and the approximations used, the initial preparation and its coherence, the location of the target node, site energies, static disorder, noise, dissipation, etc. In this context, optimality refers to several transport features as absence of losses, short required time, and robustness (regardless of sudden changes of working conditions). One hindrance to optimal transport is represented by the presence of *dark* or *invariant subspaces/states* [7]. Inspired by the similar use of the term ‘dark states’ in quantum optics [18] and condensed matter physics [19, 20], Caruso *et al* [7] defines them as Hamiltonian eigenstates that have no overlap with the ‘target’ node on the network. They, hence, act as a trap on the network blocking transport. Then, transport efficiency can be increased by either avoiding the dark subspace, or applying certain techniques to nudge states out of the dark subspace, or by destroying the subspace [21–24]. Here, we will discuss these different methods to enhance quantum transport by means of graph theoretical tools, and apply them to describe the energy transport behaviour that has been recently experimentally observed for a bio-engineered light-harvesting complex realized on a cylinder (M13 virus) structure [25].

This paper is structured as follows. In section 2, we formally introduce the network, its dynamics and the corresponding dark subspace. Section 3 reviews methods that are used to enhance (energy) transfer on quantum networks through the lens of dark states: initialisation outside of the dark subspace, using control fields, and coupling with the environment thus introducing noise and disorder. In section 4, we employ graph theoretical results in order to find two results on the dark subspaces on graphs: that there exist dynamics having no associated dark subspace, and that very large graphs asymptotically almost surely have no dark subspace. In section 5 we describe some applications of these studies to light-harvesting complexes. Finally, in section 6 we illustrate the results numerically by changing the underlying topology of two specific networks, one of which is inspired by a recent experiment with genetically-engineered light-harvesting structures [25]. We also highlight the importance of dephasing noise to enhance the transfer efficiency. Some conclusions are drawn in section 7.

2. Quantum network

A quantum network consists of an underlying graph, on which the dynamics is described via quantum mechanics, as opposed to the usual transition matrices or hopping dynamics of classical networks [26]. A graph, $G = (V, E)$, consists of a set of vertices or nodes $V(G)$ and a

set of edges $E(G)$. Let $N = |V(G)|$ be the number of nodes on the graph. The graph can be described by its adjacency matrix $A(G)$, defined as

$$[A(G)]_{ij} = \begin{cases} \alpha_{ij}, & \text{if } (i,j) \in E(G); \\ 0, & \text{otherwise,} \end{cases} \quad (1)$$

where $i, j \in V$ are nodes of the network, and α_{ij} are the weights of the edges. We consider the edges to be undirected and without loops, unless specified otherwise. The coherent dynamics is described by the Hamiltonian:

$$H_0 = \sum_{i=1}^N \hbar\omega_i \sigma_i^+ \sigma_i^- + \sum_{i \neq j} \hbar [A(G)]_{ij} (\sigma_i^+ \sigma_j^- + \sigma_j^+ \sigma_i^-), \quad (2)$$

where σ_i^+ and σ_i^- are the raising and lowering operators at node i respectively, $\hbar\omega_i$ is the local site energy, and $[A(G)]_{ij} = \alpha_{ij}$ determines the hopping rate (interaction) between joined nodes i and j .

In the following we will consider the single excitation approximation, as often used for light-harvesting complexes and for quantum states and information transfer [7, 27, 28]. Hence, the state $|i\rangle$ denotes the presence of one excitation in node i , i.e. $\sigma_i^+ = |i\rangle\langle 0|$, etc. The exit or target node can be thought of as the location from which a decay process transfers irreversibly excitation to a sink, labelled as $N+1$. If the target node is node N , then this decay can be formally described by the addition of the Lindblad superoperator

$$\begin{aligned} \mathcal{L}_{sk}(\rho) \\ = \Gamma_{N+1} (2\sigma_{N+1}^+ \sigma_N^- \rho \sigma_N^+ \sigma_{N+1}^- - \{\sigma_N^+ \sigma_{N+1}^- \sigma_{N+1}^+ \sigma_N^-, \rho\}), \end{aligned} \quad (3)$$

where ρ describes the state of the network, Γ_{N+1} is the decay rate to the sink, and $\{A, B\} = AB + BA$ is the anti-commutator. The transfer efficiency is given by the probability of population transfer to the final node:

Definition 1. Consider a graph G with Hamiltonian dynamics H_0 , network state ρ , target node N and sink decay Γ_{N+1} . The *transfer efficiency* is

$$p_{\text{sink}}(t) = 2\Gamma_{N+1} \int_0^t \rho_{NN}(s) ds. \quad (4)$$

Formally, the transfer efficiency represents the probability for the electronic excitation to be transferred to the sink, while $1 - p_{\text{sink}}(t)$ corresponds to the *energy trapped* in the network.

When all the sites have the same local energies and coupling energies, these networks resemble those studied in the field of quantum search with continuous time quantum walks [29, 30]. There also exists contrasting quantum networks with discrete-time evolution that can be written in a quantum circuit formulation [31, 32] which we are not considering here. However, it should be noted that continuous-time quantum walks and discrete-time quantum walks are connected by a limiting procedure, as it is shown in [33].

Now, we consider the following definition of dark subspace [7]:

Definition 2. Consider a graph G with Hamiltonian dynamics H_0 and target node N , corresponding to the state $|N\rangle = (0, 0, \dots, 0, 1)$ in the site basis. The *dark subspace* is the vector space spanned by the eigenvectors of H_0 that are orthogonal to $|N\rangle$.

In order to determine the dark states, it is necessary to know the spectrum of the Hamiltonian and the position of the exit node. The term ‘dark state’ in this context was first used by [7],

who called the dark subspace as the ‘invariant subspace’, since it is invariant under the dynamics described above. We can also define the corresponding *light subspace* as being spanned by all the eigenvectors of H_0 that are not orthogonal to the target node $|N\rangle$. In this last set of eigenvectors it is possible to identify a particular subset made of quasi-dark states that are quasi-orthogonal to $|N\rangle$:

Definition 3. Consider a graph G with Hamiltonian dynamics H_0 and target node N , corresponding to the state $|N\rangle = (0, 0, \dots, 0, 1)$ in the site basis. The *quasi-dark states* are eigenvectors $\{|\psi\rangle\}$ of H_0 where $|\langle N|\psi\rangle| \leq \epsilon$.

Quasi-dark states do not trap the excitation permanently as dark states, but they can cause transport to be slow, where the value of ϵ will depend on the preferred time and energy scale in a particular application. More generally, we can quantify the trapping capacity of an eigenvector with the darkness strength:

Definition 4. Consider a graph G with Hamiltonian dynamics H_0 and target node N , corresponding to the state $|N\rangle = (0, 0, \dots, 0, 1)$ in the site basis. Let $|\phi\rangle$ be an eigenvector of H_0 . The *darkness strength* ε of $|\phi\rangle$ is $|\langle N|\phi\rangle| =: \varepsilon$.

The darkness strength is zero for dark states and very close to zero for quasi-dark states.

In the case of noisy quantum dynamics, that is the network is coupled to some environment, then there can be also dissipative and dephasing processes. They can be described by the following Lindblad superoperators,

$$\mathcal{L}_{\text{diss}}(\rho) = \sum_{j=1}^N \Gamma_j \left(2\sigma_j^- \rho \sigma_j^+ - \left\{ \sigma_j^+ \sigma_j^-, \rho \right\} \right), \quad (5)$$

$$\mathcal{L}_{\text{deph}}(\rho) = \sum_{j=1}^N \gamma_j \left(2\sigma_j^+ \sigma_j^- \rho \sigma_j^+ \sigma_j^- - \left\{ \sigma_j^+ \sigma_j^-, \rho \right\} \right), \quad (6)$$

where Γ_j and γ_j are dissipation and dephasing rates for node j , respectively. The total evolution of the state of the network is then

$$\begin{aligned} \dot{\rho}(t) \\ = -\frac{i}{\hbar} [H_0, \rho] + \mathcal{L}_{sk}(\rho) + \mathcal{L}_{\text{diss}}(\rho) + \mathcal{L}_{\text{deph}}(\rho) \equiv \mathcal{L}[\rho], \end{aligned} \quad (7)$$

where \mathcal{L} is the Lindblad superoperator that describes the coherent and incoherent part of the system evolution and $[A, B] = AB - BA$ is the commutator.

Further on in the paper for specific illustrative cases (especially sections 3.3 and 6), we will consider homogeneous and non-weighted graphs:

Definition 5. A graph G is *homogeneous* when every node in $V(G)$ has the same properties: the same local energy $\hbar\omega_j = \hbar\omega$, the same dissipation rate $\Gamma_j = \Gamma$ and the same dephasing rate $\gamma_j = \gamma \forall j \in V(G)$. Furthermore, if the weights of the edges $\alpha_{ij} = a \forall (i, j) \in E(G)$ then G is also a *non-weighted graph*.

2.1. Examples of dark subspaces

In the homogeneous case and uniform coupling rates, the Hamiltonian H_0 in the single excitation subspace is the adjacency matrix of the underlying network. Thus, the dark subspaces

of the Hamiltonian are the eigenspaces of the network that are orthogonal to $(0, \dots, 0, 1)$. Non-degenerate eigenvalues with eigenvectors of form $(\dots, 0)$ lead to one-dimensional dark subspaces, while eigenvalues with degeneracy k are related to dark subspaces of at least dimension $k - 1$, depending on whether or not the eigenspace is entirely orthogonal to the target node—see appendix in [7] to see how to find them.

We can consider the more general question of whether a network has any potential dark subspaces—whether it has any eigenvectors with zero entries in the site basis. Clearly, networks with degenerate eigenvalues will automatically have dark subspaces relative to any node of the network. In terms of substructures, it has been found that 0 and -1 eigenvalues are related to stars and cliques on the network [34–36], suggesting that graphs with many stars or cliques will have degenerate 0 or -1 eigenvalues, respectively.

Now, we look at some examples of dark subspaces on paths, lattice graphs and complete graphs [7, 15]. However, by exploiting the knowledge of the eigenspectrum of numerous other classes of graphs [37], our statements about the corresponding dark subspaces can be generalized to other complex networks.

- **Path and Lattice Graphs:** State transfer on spin chains and spin networks have been studied in the literature (e.g. [1, 4]), and they are one of the fundamental models in physics. Underlying spin chains with nearest neighbour coupling are path graphs. The eigenvalues of path graphs are all nondegenerate $\lambda_k = 2 \cos(\pi k / (N + 1))$ for $k = 1, \dots, N$. The corresponding unnormalised eigenvectors x_k have components $(x_k)_m = \sin(\pi m k / (N + 1))$ and zeros emerge at ‘symmetry points’ that split the path graph into equal parts [37]. Thus, if our target node is at any one of these zeroes, then there is a dark subspace. However, in typical state transfer on spin chains, the target node is the end node, where there is never a zero: hence perfect state transfer is clearly possible because there is no relevant dark subspace. Larger lattice graphs also have dark nodes at symmetry points of the network [15, 38].
- **Complete Graphs:** A fully connected network (FCN), or complete graph, of N nodes, is defined as a network where there is a link between any pair of nodes. There is one eigenstate $|\phi\rangle = (1/\sqrt{N}) \sum_{j=1}^N |j\rangle$ with eigenvalue $\lambda_1 = N - 1$, and a degenerate eigenspace of dimension $N - 1$ with eigenvalue $\lambda_2 = \dots = \lambda_N = -1$ [37], whose basis can be chosen as $|\psi_j\rangle = |1\rangle - |j\rangle$ for $j = 2, \dots, N$. The dark subspace is spanned by $\{|\psi_j\rangle : j = 2, \dots, N - 1\}$, which has dimension $N - 2$. If the initial state is localised on a single node, then it is unavoidable that a component of it will lie in the dark subspace [7].

3. How to enhance transfer

In this section, we review several tools that can be exploited in order to increase the network transfer efficiency. One could either choose specific initial states, as in section 3.1, or use control fields to time-dependently change the effective Hamiltonian dynamics as in section 3.2. Section 3.3 considers the case where disorder and dephasing are applied to the system dynamics.

3.1. Smart initialisation

The evolution of the eigenstates in dark subspace is coherent and stationary (up to a phase), hence it will never lead to a state with a non-vanishing component on site N , i.e. without reaching the exit node N . Indeed, the evolution of the dark subspace as a whole is also invariant.

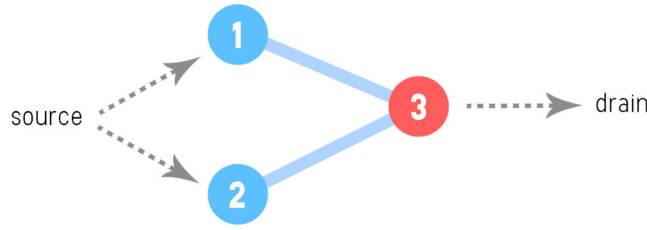


Figure 1. Trimer configuration. The source can either initialise the state as an incoherent mixture of $|1\rangle$ and $|2\rangle$ or as a coherent superposition of $|1\rangle$ and $|2\rangle$.

If the initial state on the network has any non-zero component in the dark subspace, that component remains within the dark subspace and thus forever trapped on the network. Only the components in the corresponding light subspace will transfer to the exit. By initialising completely *outside* the dark subspace, i.e. with an initial state that is orthogonal to the dark subspace, full transfer of the energy will eventually occur:

$$\lim_{t \rightarrow \infty} p_{\text{sink}}(t) = 1. \quad (8)$$

However, the transfer can still take a long time if there are any quasi-dark states.

This line of attack is pursued by [7, 39], who consider small networks with three nodes known as trimers, shown in figure 1. Trimers have one dark state that causes excitations to get trapped [7, 20, 40–43]. In fact, one can consider the following Hamiltonian (in the first excitation subspace),

$$H = \begin{bmatrix} 1 & 0 & 1 \\ 0 & 1 & 1 \\ 1 & 1 & 1 \end{bmatrix}, \quad (9)$$

with the target node being $|3\rangle = (0, 0, 1)$. Hence, the dark state is $|D\rangle = (|1\rangle - |2\rangle) / \sqrt{2}$, and the other two eigenstates are $1/2 (|1\rangle + |2\rangle) \pm \sqrt{2}/2|3\rangle$. If the network state is initialised as $|1\rangle$ or $|2\rangle$, or in an incoherent combination, then the state is inevitably partly trapped in the dark state. Conversely, if the initial state is the coherent superposition $(|1\rangle + |2\rangle) / \sqrt{2}$, then perfect transfer occurs. For the in-between initialisation $(|1\rangle + e^{i\phi}|2\rangle) / \sqrt{2}$, there is imperfect transfer, with zero transfer when $e^{i\phi} = -1$ (i.e. initialisation as the dark state). There, dephasing in conjunction with smart initialisation (see section 3.3) is required to suppress the dark state. This holds for more general networks—if the initial state is completely within the light subspace then the asymptotic transport efficiency is unity.

However, since eigenstates tend to be delocalized and a generic initial superposition will necessarily have a non-zero component in the dark subspace, other techniques will be exploited later to enhance transport.

3.2. Control fields

Applying various control fields on the network during the transfer process could alter the direction of the evolution of the state of the network, and increase transport efficiency by modifying the nature of the dark subspace.

Given a controlled system, a state ρ' is reachable from state ρ_0 if there is a sequence of control fields (along with any underlying Hamiltonian evolution) that will evolve ρ_0 into ρ' in some finite time. A system is *controllable* (or *fully controllable* [44]) if any state in the

state space is reachable from any other state [6, 45]. Formally, if H_0 is the system/network Hamiltonian (that is time-independent), H_m are a set of Hamiltonians that can be applied onto the network, and $f_m(t)$ are the time-varying controls, then the total Hamiltonian under which the system evolves is

$$H(t) = H_0 + \sum_m H_m f_m(t). \quad (10)$$

A system is fully controllable if the Lie algebra rank condition is true: if the Lie algebra generated by iH and iH_m is isomorphic to unitary group $u(N)$ [44], generating all possible unitaries.

Pemberton–Ross *et al* [6] find that the more *symmetric* a network is, the larger the dark subspace tends to be; by adding controls, modifying the Hamiltonian etc, these symmetries can be broken and some dark states can be accessed. In [46], symmetry breaking is used to make a controlled quantum thermal switch. When the switch is ‘off’, the central qubits are all in the dark subspace and no energy can be transferred from one side to the other. Zimborás [47] breaks time-reversal symmetry to increase transport efficiency. More generally [48, 49], study how symmetries of the Hamiltonian relate to lack of full controllability, and [50] finds that lack of certain symmetries of the Hamiltonians are necessary for full controllability.

Control fields could also take the network into a higher excitation subspace. By doing so, [6] define two grades of dark states: weaker dark states that become non-dark by the introduction of extra excitations or energy-preserving control fields; and *truly dark states* that require permutation symmetry-breaking⁷ to be destroyed. As such, the weaker dark states could be used as *storage*, since they are more protected from decay (from the sink) than the non-dark states, and are more accessible than the truly dark states [6].

The application of control fields is often not desirable, however. A static network that has high transfer efficiency is generally simpler to implement. Since the breaking of symmetry can lead to enhanced transfer, one can indeed add randomness or dissipative dynamics to break symmetry and assist transport [7].

3.3. Disorder and dephasing

In this subsection we consider the use of disorder and dephasing on the specific case of a homogeneous fully connected network with coupling rates $\alpha_{ij} = 1$, which was studied by [7]:

Definition 6. A graph G with adjacency matrix $A(G)$ is said to be a *fully connected network* (FCN) if there is an edge between every pair of nodes: $[A(G)]_{ij} \neq 0$ for all $i \neq j$.

In our particular case the corresponding adjacency matrix is:

$$[A(G)]_{ij} = \begin{cases} 1, & \text{if } i \neq j; \\ 0, & \text{otherwise.} \end{cases} \quad (11)$$

Caruso *et al* [7] find that the probability of transfer for a homogeneous FCN of size N is:

$$p_{\text{sink}}(\infty) = \frac{1}{N-1}, \quad (12)$$

i.e. for large networks the transfer is very small. In fact, such perfectly coherent networks are even worse than classical networks with incoherent hopping which have *complete* transfer in the limit $t \rightarrow \infty$. The poor transfer can be seen as being due to the large size of the

⁷Permutation symmetry-breaking would involve unequal control fields or disorder such that the interchange of previously indistinguishable qubits is now invalid.

dark subspace, given the network symmetries intrinsic in the complete graph with identical nodes—in fact, it has the largest possible dark subspace of dimension $N - 2$ for a network of N nodes. By introducing *static disorder* to D local node energies, the dark subspace reduces in size and the probability increases to

$$p_{\text{sink}}(\infty) = \frac{1}{N - D - 1}. \quad (13)$$

Hence, for a FCN with $D = N - 2$ different (disordered) node energies, $p_{\text{sink}}(\infty) = 1$. Any initial state has no component in any remaining invariant subspace [7]. Static disorder can also make transfer more robust against dissipation/noise in the weak dissipation regime [51].

Local dephasing on the network nodes has a very similar effect. If there is local dephasing on *all* nodes then the dark subspace can vanish, and $p_{\text{sink}}(\infty) \rightarrow 1$. In the special case of FCN the best method to obtain a unity transfer efficiency in short times is to apply strong dephasing, which leads to complete lack of coherence and so to a classical dynamics; this is due to the large size of the dark subspace, as discussed before. Instead, other networks need an interplay between quantum coherence and dephasing to destroy the invariant subspace and to obtain the same performance of FCN in the classical regime [7, 15]. The time evolution of the transfer efficiency in case of static disorder and local dephasing are shown in figure 2, for a FCN with $N = 32$ nodes. For simplicity's sake and for illustration purposes, the sink rate is taken to be $\Gamma_{N+1} = 1$. In fact, as it has been demonstrated in [7], $\Gamma_{N+1} \approx 1$ gives rise to similar behaviour; conversely, if $\Gamma_{N+1} \ll 1 \vee \Gamma_{N+1} \gg 1$, $p_{\text{sink}}(\infty) \rightarrow 0$, independently from any other boundary conditions. The fact that for large Γ_{N+1} the transfer to the sink is very low is due to quantum Zeno phenomena. Furthermore we set the dissipation rates $\Gamma_j = 0$ for $j = 1 \dots N$ as environment-induced dissipation can enhance transport if pure dephasing or static disorder are present [7] and we currently wish to isolate the effects of static disorder and pure dephasing. Note that the transfer efficiency has been averaged over the location of the sink, since especially in asymmetric cases, different sink locations give rise to different dark subspaces.

Dephasing also leads to line broadening, i.e. another way to view the enhanced transport is due to the stronger overlap between excitation lines of the interacting nodes [7]. With the combination of dephasing and static disorder, static disorder is only advantageous when dephasing is weak. When noise (dissipation or dephasing) is too strong, quantum Zeno phenomena occur and the dynamics is frozen [7, 15, 24, 51]: this may be exploited for storage.

4. Graph theorems

For uniform site energies and coupling rates, i.e. $H = A$, we can apply two theorems from graph theory which ultimately give the existence of network dynamics for which there are *no* dark subspaces. The first result is based on the following theorem. Given a real symmetric matrix $A = [a_{ij}]$ of size N , one can always associate a weighted graph G with N nodes and with edges $\{i, j\}$ that have weights a_{ij} for $i \neq j$.

Theorem 1 (Monfared and Shader [52]). *For a given connected graph G of N vertices, and given a set of distinct values $\lambda_1, \lambda_2, \dots, \lambda_N$, there exists a real symmetric matrix A whose graph has the same topology as G and whose eigenvalues are $\lambda_1, \lambda_2, \dots, \lambda_N$, such that none of the eigenvectors of A have a zero entry.*

By the above theorem, if we have some given underlying connected topology given by graph G , then we can find a set of weightings for the edges—interactions between the different nodes—such that the corresponding adjacency matrix $A(G)$ of the graph has distinct

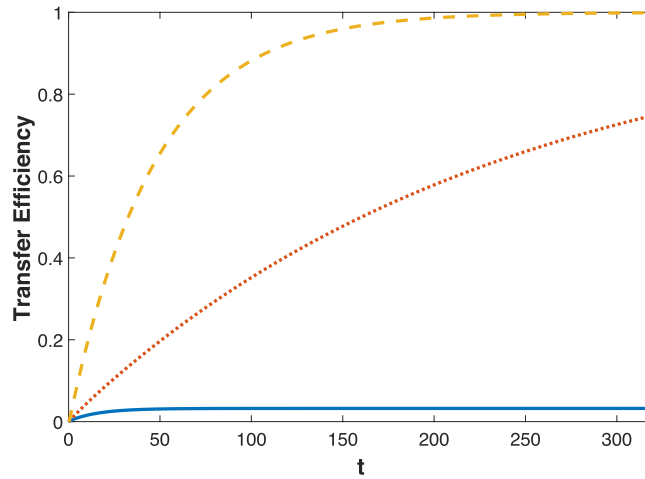


Figure 2. Transfer efficiency as a function of time, in the case of FCN with $N = 32$ nodes. Different noise conditions are shown: no dephasing (continuous line), classical dynamics (dashed) and the optimal dephasing rate between these two last regimes (dot). The transfer efficiency has been averaged over all possible input and output nodes. We have considered $\Gamma_j = 0$ for $j = 1 \dots N$ and $\Gamma_{N+1} = 1$.

eigenvalues, and all the corresponding eigenvectors have no zero entry. With such dynamics, there is no dark subspace on the network relative to any target node.

Corollary 1. *For any given underlying connected graph G , there exists Hamiltonian dynamics with no degenerate eigenvalues on the graph for which there is no dark subspace.*

Real networks tend to have eigenvalues with higher multiplicities (degeneracy) than comparable randomly generated networks [53]. However, if we are able to change the interactions between the nodes that are joined, using, for example, a combination of a different underlying Hamiltonian, control fields, and disorder and noise (see sections 3.2 and 3.3), then we could break unfavourable symmetries and we can eliminate the dark subspace altogether and achieve perfect energy transfer. In addition, our next result ultimately states that we may not even need to consider weighting the edges if the graph in question is sufficiently large.

Erdős–Rényi graphs $G(N, p)$ have N nodes, in which any edge between any two nodes has some probability p of being there [54]. These graphs are very likely⁸ to be disconnected if $p < \ln(N)/N$ i.e. if the probability of edges is sufficiently low [55]. Note that for $p \neq 0, 1$, the set of all $G(N, p)$ graphs is equivalent to the set of all graphs, since any graph will be an instance of an Erdős–Rényi graph. Given this fact, we can use the following theorem to subsequently make a statement about all asymptotically large graphs:

Theorem 2 ([56]). *A graph $G(N, \frac{1}{2})$ is controllable with probability at least $1 - CN^{-\alpha}$, for any α , where $C > 0$.*

This theorem was conjectured by [57] (see also [58]), and proven by [56]. The notation of controllability is the same as that introduced in section 3.2, i.e. the graph is controllable if the dynamics (determined by the adjacency matrix, which is equivalent to the Hamiltonian) can evolve any state into any other state on the graph. Stated in another way, theorem 2 implies

⁸ A property P of a graph holds *asymptotically almost surely* for $G(N, p)$ if the probability of P being true goes to one as $N \rightarrow \infty$.

that the relative number of controllable graphs to any graph tends to one as $N \rightarrow \infty$. By picking a very large graph at random, it is almost surely controllable, and thus almost surely has no dark states.

Corollary 2. *A connected graph G of size N , with Hamiltonian dynamics given by the adjacency matrix, asymptotically almost surely has no dark subspace as $N \rightarrow \infty$.*

Hence almost surely, energy transfer on large graphs will happen perfectly if we allow for time $t \rightarrow \infty$, without requiring the addition of further controls or different interaction strengths between the nodes. In conjunction with theorem 1, this confirms the intuition that large random graphs are generally not symmetric and tend to have distinct eigenvalues. Furthermore, the eigenvectors are noisy and delocalised, therefore leaving almost surely no place for a dark subspace to hide.

5. Application to light-harvesting

Real quantum networks are always subjected to noise. However, environmental interaction can *enhance* transport through a dissipative network⁹. Such noise can maintain and even generate quantum coherence and entanglement [60–64]. This is well demonstrated with the transport of excitations in light-harvesting complexes, which have attracted much interest in the last decade.

Light-harvesting complexes, or antenna systems, are networks composed of chromophores absorbing photons and transporting the created electronic excitations to the reaction centre (the target node). The simplest light-harvesting complex is the Fenna–Mathews–Olson (FMO) complex (found in green sulphur bacteria), and recent experimental evidence strongly suggests that quantum coherence features play a crucial role during the energy transport process [8–10].

Theoretical studies of the FMO complex show that the additional presence of dephasing noise is needed to describe the observed transport efficiency of almost 100% [7, 12–14, 65, 66]. This is further supported by the experimental study in [25], which experimentally showed that optimal transport in an engineered light-harvesting complex occurred when quantum coherence was combined with noise. There, a light-harvesting antenna system has been realized with a biological material, the M13 virus, and a chromophore network has been created on its filaments. Two versions of this system have been genetically planned: one with a network made of weakly coupled chromophores, and the other one with reduced inter-chromophoric distance, causing clusters of strongly coupled chromophores. In this second version, involving coherent and incoherent features, they have observed a remarkable improvement of both transport speed and diffusion length of the electronic excitation. The average chromophoric distance was exploited to study and control the optimal mixing rate between coherence and noise. Here, the environment assists the transport by suppressing the dark subspaces or inducing interaction between them and other states, causing ultimate leakage into the sink [7, 51].

6. Topology robustness

In this section, we numerically study the change of the dark subspaces under modifications of the quantum network. Firstly we will consider the addition of control fields across the

⁹Noise enhancement also occurs within classical mechanics, but via physically different mechanisms (e.g. stochastic resonance [59]).

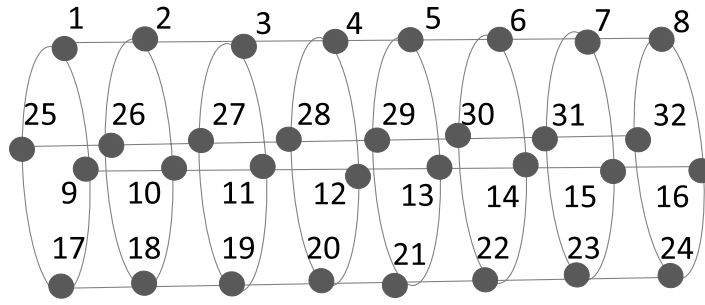


Figure 3. Diagram of the cylinder network structure.

network. A second method to modify the interactions between the nodes (with the aim to decrease the subspace) is to remove certain edges or links on the network entirely. Depending on the experimental set-up, this could decrease the experimental load, or mimic the case of material defects that lead to missing connections between nodes.

Inspired by light-harvesting complexes, we examine two different models: the fully connected network (FCN) (see definition 6) and a cylinder graph. The former suits better the antenna systems, that are typically fully connected (albeit with differing interaction energies), and the latter’s topology is similar to the M13 virus structure.

Definition 7. A graph G with adjacency matrix $A(G)$ and N nodes is said to be a *cylinder graph* if G is topologically equivalent to the Cartesian product of a path graph P_k and a cycle graph $C_{N/k}$, $P_k \square C_{N/k}$. Note that the nodes of $P_k \square C_{N/k}$ consist of $V(P_k \square C_{N/k}) = (p, c) | p \in V(P_k), c \in C_{N/k}$. An edge exists $((p_i, c_k), (p_j, c_l)) \in E(P_k \square C_{N/k})$ if either $(p_i, p_j) \in E(P_k)$ or $(c_k, c_l) \in C_{N/k}$.

Figure 3 shows a diagram of a cylinder graph. For a cylinder of dimensions $m \times n$, with m as the number of nodes along the direction orthogonal to the axis and n as the number of nodes along axis direction, the entries above the main diagonal of the $(m \times n) \times (m \times n)$ adjacency matrix, are:

$$[\tilde{A}(G)]_{ij} = \begin{cases} 1, & \text{if } j = i + 1, i \neq kn (k = 1, \dots, m - 1); \\ 1, & \text{if } j = i + kn (k = 1, m - 1); \\ 0, & \text{otherwise.} \end{cases} \quad (14)$$

The complete adjacency matrix of the non-weighted graph results from the sum of the previously strictly upper triangular matrix and its transpose.

Because of its symmetries, the cylinder graph also has an invariant dark subspace, but of lower dimension than the fully connected network’s dark subspace; this allows a greater asymptotic value of transfer efficiency (see figure 4). Furthermore, a unital transfer efficiency in short times is obtained not in a classical regime like for the FCN (figure 2), but rather with an interplay between quantum coherence and dephasing, as we stated in section 3.3.

6.1. Applied control fields

In figure 5 we apply various different control fields to modify the weight of a single edge in the FCN and cylinder networks. The time dependent functions used to modify the weight value are a linear decreasing function of the form $\alpha = -\frac{t}{t_{\max}} + 1$, and a sinusoidal function of the form $\alpha = \left| \sin \left(\frac{k\pi}{2} \left(-\frac{t}{t_{\max}} + 1 \right) \right) \right|$, with t_{\max} as the endpoint of the time interval considered.

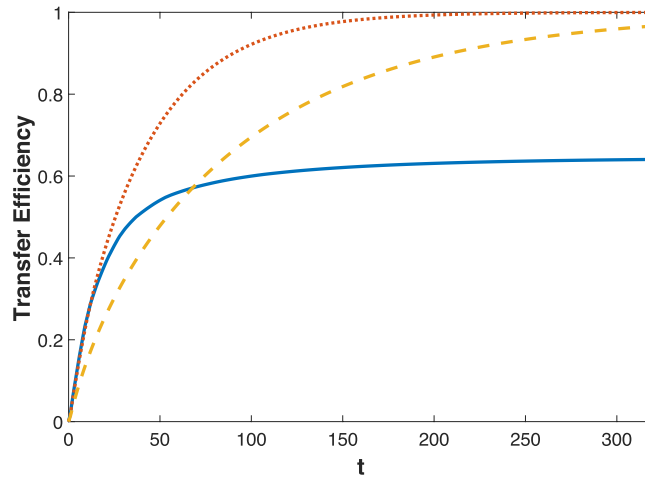


Figure 4. Transfer efficiency as a function of time, in the case of a 4×8 -cylinder with $N = 32$ nodes. Different noise conditions are shown: no dephasing (continuous line), classical dynamics (dashed) and the optimal dephasing rate between these two last regimes (dot). The transfer efficiency has been averaged over all possible input and output nodes. We have considered $\Gamma_j = 0$ for $j = 1 \dots N$ and $\Gamma_{N+1} = 1$.

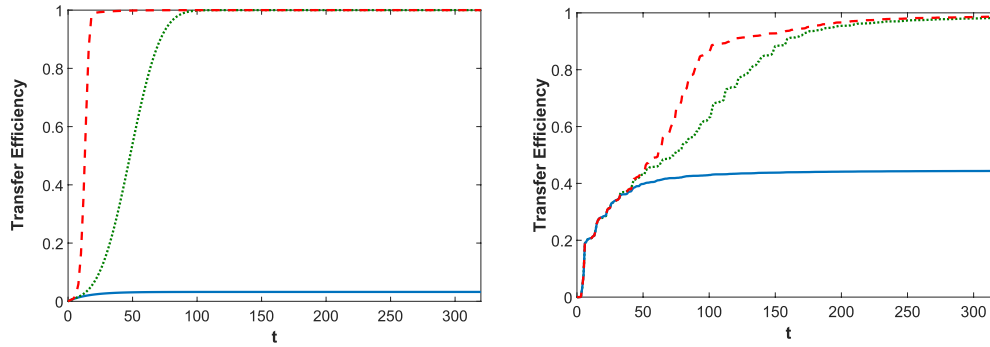


Figure 5. Transfer efficiency as a function of time, in the case of FCN with $N = 32$ nodes (left) and a 4×8 cylinder (right). Different control systems on the value of a single coupling rate $\alpha_{i,j}$ are shown: no control (continuous line), linear decrease (dot), and sinusoidal oscillation (dashed). The varying $\alpha_{i,j}$ is the coupling $\alpha_{1,32}$ in case of FCN (1 is the initial node, 32 is the node connected to the sink), while it is the coupling $\alpha_{1,9}$ for the cylinder (1 is the initial node, 9 is one of the nodes defining the circular path—see figure 3).

Transport simulations have shown that to destroy the dark subspace and obtain a unital transfer efficiency on fully connected network we have to act on an edge involving the initial node—if the dark subspace exists, then the initial node lies appears in the set $\{|\psi_j\rangle\}$ of vectors spanning the dark subspace, and even a little perturbation of one of its coupling rates may cause a significant change in the spectrum of Hamiltonian H of the system (see section 3.3). The time it takes for complete transfer to subsequently occur depends on which edge to which other adjacent node is chosen to be time-varied. The initial node has a less important role on the cylinder graph: the dark subspace vanishes if we act on an edge involved in its symmetry. The asymmetric nature of the applied fields breaks some of the prior network symmetries.

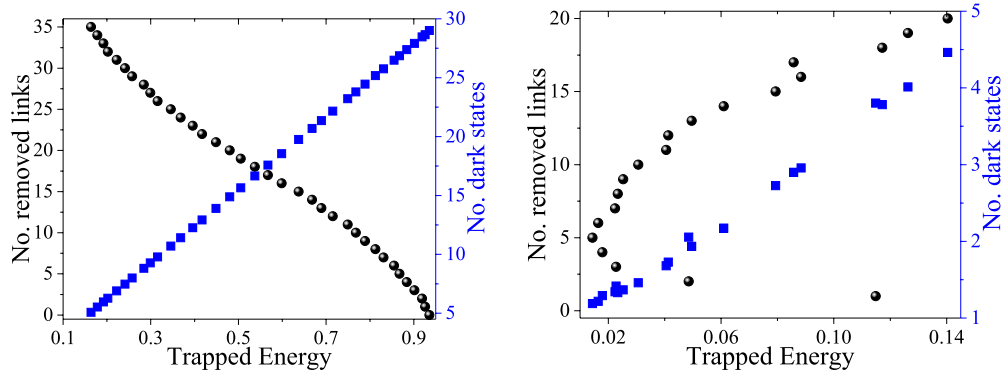


Figure 6. Relationship between the number of removed links (black spheres), the number of dark states (blue squares) and the energy trapped in the dark subspace in case of FCN (left), and 4×8 -cylinder (right); both have $N = 32$ nodes.

Furthermore, the linearly decreasing coupling field also breaks time-reversal symmetry, leading to the fast approach to complete transfer.

As previously stated in section 3.2, implementing a control system on network structure is not easy. A simpler way to enhanced transfer with a control field is by using a static network with time-dependent dephasing rates/static disorder; this topic will be analysed in a forthcoming paper.

6.2. Random removal of links

The results of randomly removing interactions between nodes is shown in figure 6. The positive effect of removing links is clear on the FCN, due to the maximally symmetric nature. Randomly removing links quickly breaks its symmetries. In turn, this leads to the reduction in the dark subspace dimension and hence reduces the amount of trapped energy. In contrast, the cylinder graph benefits from link deletion only up to a small percentage of removed links (about 5% of the total); when this percentage grows another dark subspace appears again and the transport gets worse. The energy trapped grows linearly with the number of dark states for both the FCN and cylinder networks. As the number of removed links grows, the energy trapped on the FCN network monotonically decreases, whilst the energy trapped on the cylinder network decreases initially and then increases again. The latter increase in trapped energy in the cylinder is due to the appearance of new symmetries and the increasing sparsity of the edges—while the FCN initially has 496 edges ($N(N - 1)/2$), the cylinder graph has only 60 edges (4 edges within each of the 8 cycles and 4×7 edges connecting each of the cycles successively).

However, although the deletion of links is a good method to reduce the number of dark states, it is not sufficient in reducing the presence of quasi-dark states, since the latter are more persistent. In figure 7, we plot the number of dark states and quasi-dark states as a function of the darkness strength and of the number of deleted links. Note that it turns out to be more difficult to destroy quasi-dark states by means of removing links. Moreover, in agreement with figure 6, after removing too many links in the cylinder graph, new dark states can emerge, as shown in the right panel of figure 7, which is not the case for the FCN for the number of links removed (left panel of figure 7).

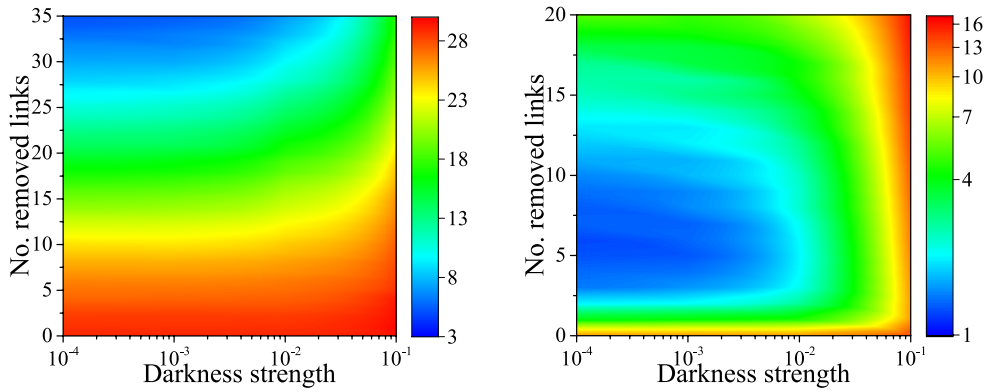


Figure 7. Number of dark states as a function of the number of removed links and the darkness strength, for FCN (left) and a 4×8 -cylinder graph (right), with 32 nodes. A similar qualitative behaviour is observed for larger networks.

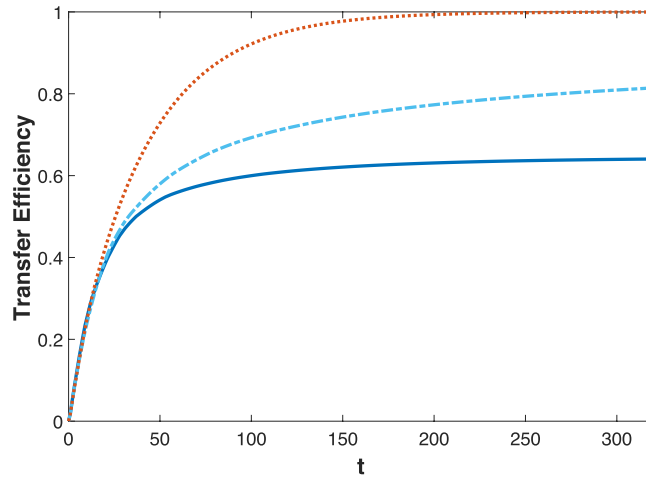


Figure 8. Time evolution of the transfer efficiency for a 4×8 -cylinder of $N = 32$ nodes in three different conditions: optimal dephasing noise with no removed links (dot line), coherent dynamics with no removed links (continuous), and coherent dynamics but with 5 removed links (dot-dashed). Each transfer efficiency has been averaged over all possible input and output states, and with $\Gamma_{N+1} = 1$.

A more subtle method of changing the node interactions is to introduce dephasing into the dynamics. In figure 8, we plot the time evolution of transfer efficiency of a cylinder graph, comparing the transfer efficiency when there are no removed links, versus with an optimal number of removed links (corresponding to minimal trapped energy of figure 6), versus the introduction of dephasing dynamics (but no removed links). In this context, dephasing noise opens up additional pathways from the initial node to the final one and therefore suppresses both dark states and quasi-dark states. The presence of noise is more effective than link deletion for transport improvement. As already discussed above, without link deletion we have a dark subspace obstructing electronic excitation from reaching the sink whilst removing 5 links allows us to obtain $p_{\text{sink}}(\infty) = 1$. If the aim is instead the achievement of an optimal

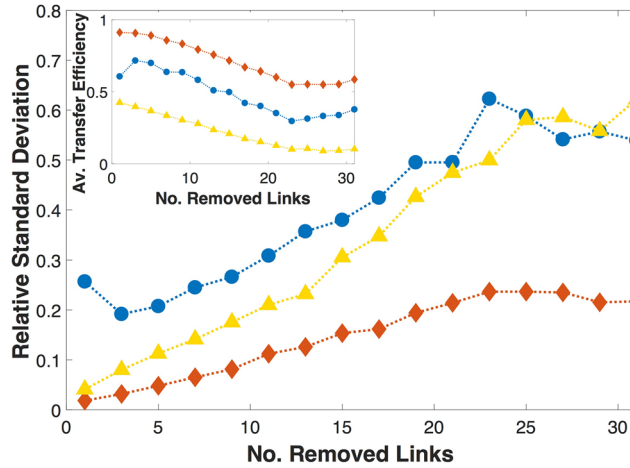


Figure 9. Relative standard deviation of transfer efficiency as a function of the number of removed links for a 4×8 -cylinder with $N = 32$ nodes, with fixed input and output nodes (at opposite ends) and $\Gamma_{N+1} = 1$, and corresponding to a sample of 200 different geometries. The corresponding averaged transfer efficiency is shown in the inset.

fast transport, dephasing noise plays a crucial role: in fact p_{sink} reaches unity in a much shorter time scale (dot line in figure 8).

Noise-assisted transport is characterized not only by a reduced time scale for the energy transfer, but also by the robustness against possible changes of the underlying topology, as discussed in [15]. By varying the geometry and adding the right amount of noise, a very good transport performance is guaranteed. This does not occur in the fully coherent and incoherent cases, where the transfer efficiency quickly decreases, as it can be seen in the inset of figure 9. This remarkable robustness is present in the regime of noise-assisted transport, as shown by the smaller dispersion around the optimal efficiency with respect to the fully coherent and incoherent regimes. Finally, let us point out that the minimum of the relative standard deviation and the maximum of the average of the transfer efficiency in the coherent case (corresponding to 5% of removed links) is a further sign of dark subspace suppression.

7. Conclusions

The dark side of quantum networks is an antagonist to optimal energy transfer. Different tools can be employed to deal with the dark subspaces: we can avoid them using smart initialisation, or suppress and destroy them by breaking the network symmetries through the use of control fields, noise, or disorder. Indeed, dark subspaces have a deep connection with topological symmetries, and can grow in size on more symmetric networks (associated to more degenerate adjacency matrices). The FCN network, for example, has the most symmetries possible on a network and hence the largest dark subspace. At the same time, the FCN network also responded most favourably to dark space suppression tools as opposed to the less symmetric cylinder graph. Whilst the dark subspace has been defined in relation to the eigenstates of the Hamiltonian describing the dynamics on the network, the framework of the dark subspaces could also be generalised to include other features, such as impurities that trap and cause decay of energy on the network [43], and to Lindbladian eigenstates in more generality. The best method to get optimal transport would depend on the function of the device we want to

plan: if the goal is the unity of p_{sink} without time limits, then designing a proper weighted network could be the solution (assuming that it is within our engineering ability); if short times and performance robustness are crucial (as it is usually the case), then the introduction of noise in the dynamics is required. Given that noise is unavoidable in most realistic systems, this implies that we generally do *not* need to eradicate all noise to achieve optimal transport—we just need to be able to control it to some degree.

Besides, we found that a network does not have any *truly* dark states, if the interactions can be tuned to achieve full controllability although this may not be quite feasible experimentally. If the interactions can be engineered, then this is advantageous in two ways: first, no excitation is truly trapped on the network, hence we can always be sure that full transfer will eventually occur; second, there will be ‘temporary’ dark states that could be used as energy storage. Furthermore, sufficiently large graphs almost surely have no dark states, implying that as our quantum networks grow in size (i.e. as the particular quantum technology grows in size), we are very likely to not require extensive interaction engineering to ensure full transport.

These results allow one to move further in understanding and enhancing state transfer on quantum networks [4, 27, 67]. These results can also be employed to understand other quantum processes such as electron transfer, and to designing solar energy devices (e.g. inspired by the energy transfer networks in photosynthetic complexes), and potential quantum thermal devices.

Acknowledgments

We would like to thank Joshua Lockhart, Yasser Omar, Danial Dervovic, Bryan Shader, Gabriel Coutinho and Stefano Gherardini for useful discussions. This work was supported by the EPSRC Centre for Doctoral Training in Delivering Quantum Technologies [EP/L015242/1]. FC was also financially supported from the Fondazione CR Firenze, through the project Q-BIOSCAN; SS was financially supported from the Royal Society, EPSRC, Innovate UK, BHF and NSCF.

ORCID iDs

Thao P Le  <https://orcid.org/0000-0001-6309-1753>

Filippo Caruso  <https://orcid.org/0000-0002-8366-4296>

References

- [1] Kay A 2010 *Int. J. Quantum Inf.* **08** 641
- [2] Mülken O and Blumen A 2011 *Phys. Rep.* **502** 37
- [3] Mohseni M, Omar Y, Engel G S and Plenio M B 2013 *Quantum Effects in Biology* (Cambridge: Cambridge University Press)
- [4] Christandl M, Datta N, Ekert A and Landahl A J 2004 *Phys. Rev. Lett.* **92** 187902
- [5] Aharonov L D Y and Zagury N 1993 *Phys. Rev. A* **48** 1687
- [6] Pemberton-Ross P J, Kay A and Schirmer S G 2010 *Phys. Rev. A* **82** 042322
- [7] Caruso F, Chin A W, Datta A, Huelga S F and Plenio M B 2009 *J. Chem. Phys.* **131** 105106
- [8] Engel G S, Calhoun T R, Read E L, Ahn T K, Mančal T, Cheng Y C, Blankenship R E and Fleming G R 2007 *Nature* **446** 782
- [9] Panitchayangkoon G, Hayes D, Fransted K A, Caram J R, Harel E, Wen J, Blankenship R E and Engel G S 2010 *Proc. Natl Acad. Sci.* **107** 12766

- [10] Panitchayangkoon G, Voronine D V, Abramavicius D, Caram J R, Lewis N H C, Mukamel S and Engel G S 2011 *Proc. Natl Acad. Sci.* **108** 20908
- [11] Scholes G D, Mirkovic T, Turner D B, Fassioli F and Buchleitner A 2012 *Energy Environ. Sci.* **5** 9374
- [12] Chin A W, Datta A, Caruso F, Huelga S F and Plenio M B 2010 *New J. Phys.* **12** 065002
- [13] Caruso F, Chin A W, Datta A, Huelga S F and Plenio M B 2010 *Phys. Rev. A* **81** 062346
- [14] Olaya-Castro A, Lee C F, Olsen F F and Johnson N F 2008 *Phys. Rev. B* **78** 085115
- [15] Caruso F 2014 *New J. Phys.* **16** 055015
- [16] Novo L, Chakraborty S, Mohseni M, Neven H and Omar Y 2015 *Sci. Rep.* **5** 1
- [17] Novo L, Mohseni M and Omar Y 2016 *Sci. Rep.* **6** 18142
- [18] Arimondo E and Orriols G 1976 *Lett. Nuovo Cimento* **17** 333
- [19] Brandes T and Renzoni F 2000 *Phys. Rev. E* **85** 4148
- [20] Emary C 2007 *Phys. Rev. B* **76** 161404(R)
- [21] Li Y, Caruso F, Gauger E and Benjamin S C 2015 *New J. Phys.* **17** 013057
- [22] Caruso F, Crespi A, Ciriolo A G, Sciarrino F and Osellame R 2016 *Nat. Commun.* **7** 11682
- [23] Viciani S, Lima M, Bellini M and Caruso F 2015 *Phys. Rev. Lett.* **115** 083601
- [24] Viciani S, Gherardini S, Lima M, Bellini M and Caruso F 2016 *Sci. Rep.* **6** 37791
- [25] Park H *et al* 2016 *Nat. Mater.* **15** 211
- [26] Lovász L 1993 *Bolyai Soc. Math. Stud.* **2** 1
- [27] Bose S, Casaccino A, Mancini S and Severini S 2009 *Int. J. Quantum Inf.* **07** 713
- [28] Caruso F, Huelga S F and Plenio M B 2010 *Phys. Rev. Lett.* **105** 190501
- [29] Childs A M and Goldstone J 2004 *Phys. Rev. A* **70** 022314
- [30] Portugal R 2013 *Quantum Walks and Search Algorithms* (New York: Springer)
- [31] Chiribella G, D'Ariano G M and Perinotti P 2009 *Phys. Rev. A* **80** 022339
- [32] Bisio A, Chiribella G, D'Ariano G and Perinotti P 2011 *Acta Phys. Slovaca* **61** 273
- [33] Strauch F W 2006 *Phys. Rev. A* **74** 030301
- [34] Dorogovtsev S N, Goltsev A V, Mendes J F F and Samukhin A N 2003 *Phys. Rev. E* **68**
- [35] Goh K I, Kahng B and Kim D 2001 *Phys. Rev. E* **64** 051903
- [36] Kamp C and Christensen K 2005 *Phys. Rev. E* **71** 041911
- [37] Miegheem P V 2009 *Graph Spectra for Complex Networks* (Cambridge: Cambridge University Press)
- [38] Martin-Hernandez J, Trajanovski S, Wang H, Li C and Miegheem P V 2012 Zero and non-zero eigenvector components graph matrices (unpublished)
- [39] Schijven P and Mülken O 2012 *Phys. Rev. E* **85** 062102
- [40] Michaelis B, Emary C and Beenakker C W J 2006 *Europhys. Lett.* **73** 677
- [41] Brandes T 2005 *Phys. Rep.* **408** 315
- [42] Mølmer K, Castin Y and Dalibard J 1993 *J. Opt. Soc. Am. B* **10** 524
- [43] Agliari E, Mülken O and Blumen A 2010 *Int. J. Bifurcation Chaos* **20** 271
- [44] D'Alessandro D 2007 *Introduction to Quantum Control and Dynamics* (London: Taylor and Francis)
- [45] Dong D and Petersen I 2010 *IET Control Theory Appl.* **4** 2651
- [46] Manzano D and Hurtado P I 2014 *Phys. Rev. B* **90** 125138
- [47] Zimborás Z, Faccin M, Kádár Z, Whitfield J D, Lanyon B P and Biamonte J 2013 *Sci. Rep.* **3** 2361
- [48] Polack T, Suchowski H and Tannor D J 2009 *Phys. Rev. A* **79** 053403
- [49] Sander U and Schulte-Herbrüggen T 2009 arXiv:0904.4654v2
- [50] Zeier R and Schulte-Herbrüggen T 2011 *J. Math. Phys.* **52** 113510
- [51] Wu J, Silbey R J and Cao J 2013 *Phys. Rev. Lett.* **110** 200402
- [52] Monfared K H and Shader B L 2016 *Linear Algebr. Appl.* **505** 296
- [53] Marrec L and Jalan S 2017 *Europhys. Lett.* **117** 48001
- [54] Erdős P and Rényi A 1959 *Publ. Math. Debrecen.* **6** 290
- [55] Albert R and Barabási A L 2002 *Rev. Mod. Phys.* **74** 47
- [56] O'Rourke S and Touri B 2016 *SIAM J. Control Optim.* **54** 3347–78
- [57] Godsil C 2012 *Ann. Comb.* **16** 733
- [58] Godsil C and Severini S 2010 *Phys. Rev. A* **81** 052316
- [59] Gammaitoni L, Hänggi P, Jung P and Marchesoni F 1998 *Rev. Mod. Phys.* **70** 223
- [60] Plenio M B and Huelga S F 2002 *Phys. Rev. Lett.* **88** 197901
- [61] Huelga S F and Plenio M B 2007 *Phys. Rev. Lett.* **98** 170601
- [62] Rivas A, Oxtoby N P and Huelga S F 2009 *Eur. Phys. J. B* **69** 51

- [63] Braun D 2002 *Phys. Rev. Lett.* **89** 277901
- [64] Benatti F, Floreanini R and Piani M 2003 *Phys. Rev. Lett.* **91** 070402
- [65] Mohseni M, Rebentrost P, Lloyd S and Aspuru-Guzik A 2008 *J. Chem. Phys.* **129** 174106
- [66] Plenio M B and Huelga S F 2008 *New J. Phys.* **10** 113019
- [67] Kendon V M and Tamon C 2011 *J. Comput. Theor. Nanosci.* **8** 422